DiVA
http://www.diva-portal.org

Postprint

This is the accepted version of a paper published in *Inorganic Chemistry*. This paper has been peer-reviewed but does not include the final publisher proof-corrections or journal pagination.

Citation for the original published paper (version of record):

González Miera, G., Bermejo Gómez, A., Chupas, P J., Martín-Matute, B., Chapman, K W. et al. (2017)
Topological Transformation of a Metal–Organic Framework Triggered by Ligand Exchange
Inorganic Chemistry, 56(8): 4576-4583
https://doi.org/10.1021/acs.inorgchem.7b00149

Access to the published version may require subscription.

N.B. When citing this work, cite the original published paper.

This document is the Accepted Manuscript version of a Published Work that appeared in final form in Inorganic Chemistry, copyright © American Chemical Society after peer review and technical editing by the publisher. To access the final edited and published work see https://pubs.acs.org/doi/10.1021/acs.inorgchem.7b00149

Permanent link to this version:
http://urn.kb.se/resolve?urn=urn:nbn:se:su:diva-143340

Topological Transformation of a Metal-Organic Framework Triggered by Ligand Exchange

Greco González Miera,[†] Antonio Bermejo Gómez,[†] Peter J. Chupas,[ψ] Belén Martín-Matute,[,†] Karena W. Chapman*[,ψ] and Ana E. Platero-Prats*[,ψ]*

[†] Department of Organic Chemistry and Berzelii Center EXSELENT on Porous Materials, Stockholm University, SE-10691 Stockholm, Sweden. [ψ] X-ray Science Division, Advanced Photon Source, Argonne National Laboratory, Argonne, Illinois 60439, United States.

ABSTRACT. Here we describe the topological transformation of pores a new framework in the bio-MOF-100 family (dia-c) into the known isomer (lcs) by doubling the pore volume, which occurs during post-synthesis modifications. During this transformation, re-assembling of the MOF building blocks into a completely different framework occurs, involving breaking/forming of metal-ligand bonds. MOF crystallinity and local structure are retained, as determined by powder X-ray diffraction (PXRD) and pair distribution function (PDF) analyses, respectively. We have exploited the inherent dynamism of bio-MOF-100 by coupling chemical decorations of the framework using solvent-assisted ligand exchange (SALE) to the topological change. Following this method and starting from the pristine dense dia-c phase, open lcs-bio-MOF-100 was prepared and functionalized in-situ with an iridium complex (IrL). Alternatively, the dia-c MOF could be modified with wide-ranging amounts of IrL up to ca. 50 mol%, as determined by solution 1H Nuclear Magnetic Resonance (NMR) spectroscopy, by tuning the concentration of the solutions

used and with no evidence for isomer transformation. The single-site nature of the iridium complexes within the MOFs was assessed by X-ray absorption spectroscopy (XAS) and PDF analyses. Ligand exchanges occurred quantitatively at room temperature, with no need of excess of the iridium metallolinker.

INTRODUCTION

The versatility of porous metal-organic framework (MOF) architectures and chemical compositions underlies the view that they will find important applications spanning gas storage/separation,[1-2] remediation of toxic chemicals,[3,4] drug delivery[5-7] and catalysis[8-10]. Metal ion clusters and organic ligands can self-assemble into ordered three-dimensional arrays with richly varied topologies.[11] Controlling and optimizing their structure and surface chemistry for specific uses remains a critical challenge.

The crystalline MOFs were originally envisioned as fixed atomic structures, with MOFs either retaining their structure or collapsing irreversibly under different environmental conditions. The framework chemistry and architecture were established based on how the metal ion and ligand building blocks assembled during synthesis. Subsequently, the dynamic nature of MOF structures have been recognized[16] with ordered flexing of the crystalline lattice leading to contractions and expansions of the pore network. This so-called breathing effect is often triggered by removal[17] or inclusion[18,19] of guest molecules. Recently, the potential to modify a given MOF post-synthetically, without changing the framework topology, has provided further control of their structure and functional properties. The interior surface of a MOF can be decorated by reactions with guest molecules (e.g. atomic layer deposition or through "click" chemistry).[20,21-22] In the extreme case, the native ligands can be partially replaced by chemically-functionalized variants of

the ligand[26] or indeed more extended ligands,[27-28] to incorporate new functionalities or to expand the pore volume/dimensions, while retaining the original architecture (referred to as iso-reticular). This ligand-exchange, which is typically mediated by solvent (i.e. solvent-assisted ligand exchange or SALE),[29,30] provides access to MOFs with larger pores and surface functionalities (e.g., through exchange of ligands with catalytic centers) which often cannot be prepared through conventional synthetic approaches.

The supramolecular MOF architectures have yet to realize the ultimate level of control of structure and function found in biological (e.g. DNA)[31] and biomimetic systems whereby interconversion between different assemblies occurs regularly in response to external stimuli. Discrete supramolecular systems have shown interconversion of topological isomers with the same chemical formula and atom connectivity but with different topologies (e.g. knots or catenanes).[32-33] In MOFs, transformations to different architectures have been observed in a handful of systems. However, these conversions are to denser phases with less accessible porosity, which are more energetically favorable.[34]

Bio-MOF-100 is a large pore MOF in which some of the largest isoreticular changes in framework/pore volume have been achieved through SALE.[29,27] Bio-MOF-100 (named for the biological origin of the adeninate ligand within the secondary-building units)[35] has zinc-adeninate tetrahedral building units (ZABU) connected by twisting triplet of 4,4'-biphenyldicarboxylate ligands struts (BPDC) (Figure 1). The reported bio-MOF-100 phase consists of the ZABU nodes pack into a highly open **lcs** lattice featuring hexagonal-shaped mesoporous channels of 2.8 nm diameter (Figure 2). Exchange of native ligands for longer ones in bio-MOF-100 using SALE has given a 20% increase in framework and a 50% increase in pore volume;[28] arguably the most pronounced post-synthetic modification that has been effected in a MOF.

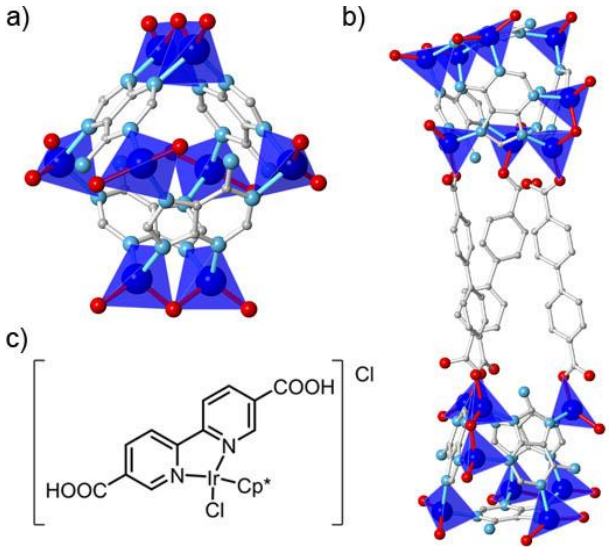

Figure 1. a) Structure of the ZABU ($Zn_8(AD)_4O_{16}$) nodes [C- grey, O- red, N-light blue and Zn blue]. b) Twisting triplex struts $(Zn_8(AD)_4O_2)_2(BPDC)_3$ in bio-MOF-100. c) Representation of the iridium complex H_2IrL used in this work to be introduced by SALE in bio-MOF-100.

Here we report a new MOF within the bio-MOF-100 family that can undergo a topological transformation to a different bio-MOF architecture with doubled pore volume. The new bio-MOF-100 is a topological isomer of the previously reported phase (**lcs** net), and adopts a catenated diamondoid **dia-c** net. The **dia-c** bio-MOF is obtained through stirred synthesis and transforms into the open-pore net when soaked in solvent at room temperature. We show that this topological transformation of bio-MOF-100 can be coupled to selective chemical decorations of the MOF scaffold. Based on previous works in our research groups on functionalization of MOFs with organometallic complexes,[23,36] we extended the use of the iridium complex, denoted as IrL (i.e. $[Cp^*Ir(BPYDC)(Cl)Cl]^{2-}$ (BPYDC = 2,2'-bipyridine-5,5'-dicarboxylate, Cp* = pentamethylcyclopentadienyl)), as a decorative motif in bio-MOF-100 using SALE methods. Alternatively, native ligands within the **dia-c** phase can be exchange by IrL complexes stochiometrically at room temperature up to 50 mol%. Framework integrity was assessed by

combined analyses of synchrotron powder X-ray diffraction (PXRD) and pair distribution function (PDF) data. The single-site nature of the iridium complexes was determined by solution ^{1}H Nuclear Magnetic Resonance (NMR) spectroscopy, X-ray absorption spectroscopy (XAS), and Pair Distribution Function (PDF) analyses.

EXPERIMENTAL SECTION

The **dia-c**–form of bio-MOF-100 was synthesized following the procedure previously reported[35] for **lcs-**bio-MOF-100 but introducing stirring to the synthesis (Yield: 135.8 mg, 15.8% based on adenine. See ESI for details). BPDC ligands within the bio-MOF-100 frameworks were exchanged with the iridium complex IrL *via* SALE methods using stirred solutions of H_2IrL in DMF at room temperature over 24 h. It is important to note that the solutions contained the absolute amount of iridium complex to be incorporated in the MOF (see ESI for details). For samples 2x5IrL and 3x5IrL, **dia-c-**bio-MOF-100 was stirred two and three times, respectively, with fresh solutions of H_2IrL in DMF targeting a 5 mol% of exchange each cycle.

The extent of IrL incorporation was quantified by ^{1}H NMR spectroscopy after digestion of the samples. Samples were suspended in a 0.04 M solution of D_3PO_4 (85% in D_2O, 5 mg) in DMSO-d_6 (1 mL) and stirred at room temperature for 10-30 minutes to allow the digestion of the MOFs. The solutions were then placed in NMR tubes. ^{1}H NMR spectra were recorded at 500 MHz on a Bruker Advance spectrometer using a BBO S2, 5 mm; BTO probe with z-gradient. The parameters of the acquisition were: number of scans: NS = 200, and relaxation delay: D_1 = 5 s.

TGA analyses were performed on the pristine and IrL-containing MOFs under N_2 flow on a Perkin Elmer TGA heating at 5 °C/min between 50-700 ºC.

Synchrotron PXRD data were collected at beamline 17-BM at the Advanced Photon Source (APS) at Argonne National Laboratory (ANL). The incident X-ray wavelength was 0.72768 Å.

Data were collected using a PerkinElmer flat panel area detector (XRD 1621 CN3/EHS) over the angular range 1-11° 2-theta. Samples were carefully ground and loaded into 1 mm diameter kapton capillaries. Cell indexing, Le Bail whole pattern fitting[37] and peak intensity extraction were performed using TOPAS software.[38] Charge flipping[39] methods implemented in Superflip[40] were applied to solve the structure of **dia-c-**bio-MOF-100. The model was refined using Materials Studio software.[41] See ESI for details concerning the structure determination of this MOF based on PXRD methods. CCDC 1502535 contains the supplementary crystallographic data. The topological analyses were performed with TOPOS software[42] following the principle of underlying nets.[43,44]

High energy X-ray scattering data suitable for PDF analyses were collected at beamline 11-ID-B at the Advanced Photon Source (APS) at Argonne National Laboratory (ANL). The PDFs, *G(r)*, were extracted from total scattering data using PDFgetX3[45] to Q_{max} = 22.5 Å^{-1}. Differential PDF (dPDF) of the IrL-containing MOFs were obtained by subtracting the contribution of the pristine material to the PDF of the sample. The area and peak position for dPDF features of interest were quantified by fitting Gaussian functions within Fityk.[46]

Ir L_{III}-edge Extended X-ray Absorption Fine Structure (EXAFS) and X-ray Absorption Near Edge Structure (XANES) experiments were carried out at beamlines 9-BM-B and 20-BM-B at the Advanced Photon Source (APS) at Argonne National Laboratory (ANL). Data were collected in fluorescence mode at 9-BM-B and in transmission mode at 20-BM-B. Data processing and analyses were performed with the Athena software package using IFEFFIT.[47,48] The EXAFS reduced data $\chi(k)$ were Fourier-transformed into R-space over the range 2–11 Å^{-1} with a k_3 weighting factor and a 3 Å^{-1} Hanning window.

RESULTS AND DISCUSSION

A new MOF was precipitated from a reaction mixture that matches the reported synthesis of bio-MOF-100[35] except, in the present case, the reaction mixture was stirred rather than left at rest. The PXRD data clearly indicated that this novel phase adopts a different atomic structure than that previously reported for bio-MOF-100, with a smaller unit cell and lower symmetry (*Cc*, *a* ~21.0 Å, *b* ~21.9 Å, *c* ~30.4 Å, *β* ~89.1° cf. *Ia-3d*, a ~69 Å) (Figure 2a). However, PDF analyses demonstrate that this phase has the same local structure as bio-MOF-100, being composed of ($Zn_8(AD)_4O_{16}$) zinc-adeninate building units (ZABU) (Figure 2b). Compositional analyses on this MOF based on ^{1}H NMR spectroscopy show a proportion of BPDC and AD ligands characteristic of bio-MOF-100. These results demonstrate the polymorphic relationship between these two bio-MOF-100 frameworks.

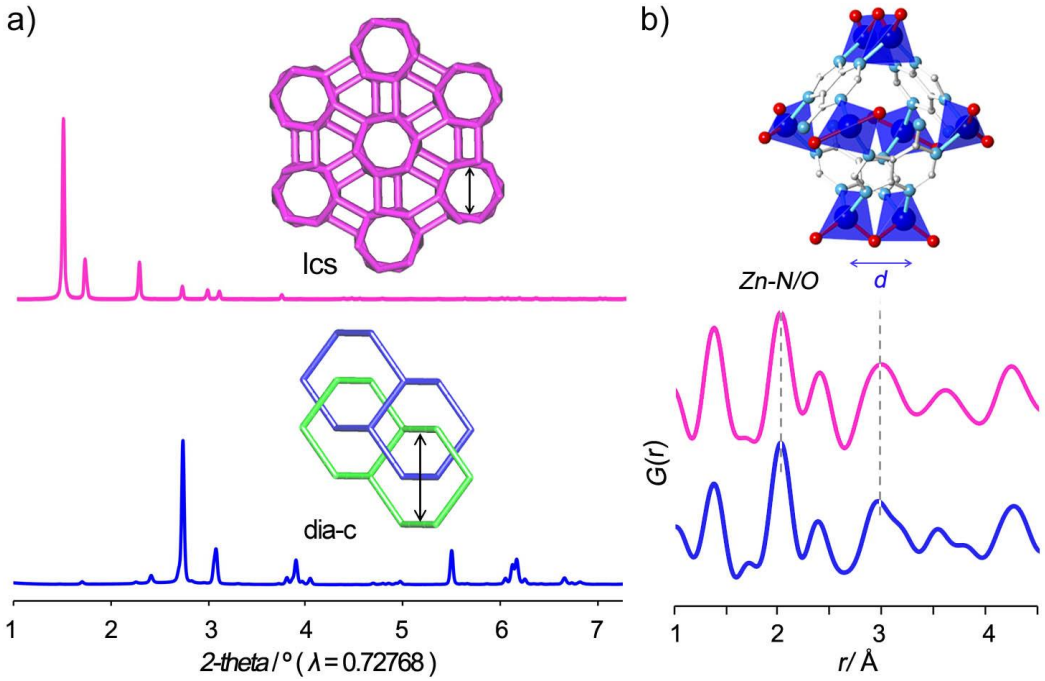

Figure 2. a) PXRD data of the bio-MOF-100 frameworks showing the occurrence of different crystalline phases (arrows point the 2.8 nm pores within the **lcs** and **dia-c** forms) and b) PDF data showing the presence of the characteristic ZABU nodes of this MOF.

The structure of this new MOF, determined from the PXRD data, has tetrahedrally-connected ZABU nodes linked by BPDC triplets as seen in bio-MOF-100. But the new MOF adopts a different framework topology. The MOF obtained from a stirred synthesis features a catenated or interpenetrated framework with two identical nets with diamond topology (**dia-c**) and pores in a chair-like conformation of 1.4 nm diameter (Figure 3a). By contrast, the bio-MOF-100 precipitated from static reaction mixtures forms a non-interpenetrated **lcs** network with pores of 2.8 nm diameter in a twist-boat conformation and with approximately half the framework density (Figure 3b). bio-MOF-100 with different compositions but the same **lcs** topology have been previously been referred to as bio-MOF-101 and bio-MOF-102.[28] Here we refer to the two MOFs as **lcs**- and **dia-c**-bio-MOF-100, for materials prepared under static and stirred reaction mixtures, respectively, which have the same framework composition but different framework topologies.

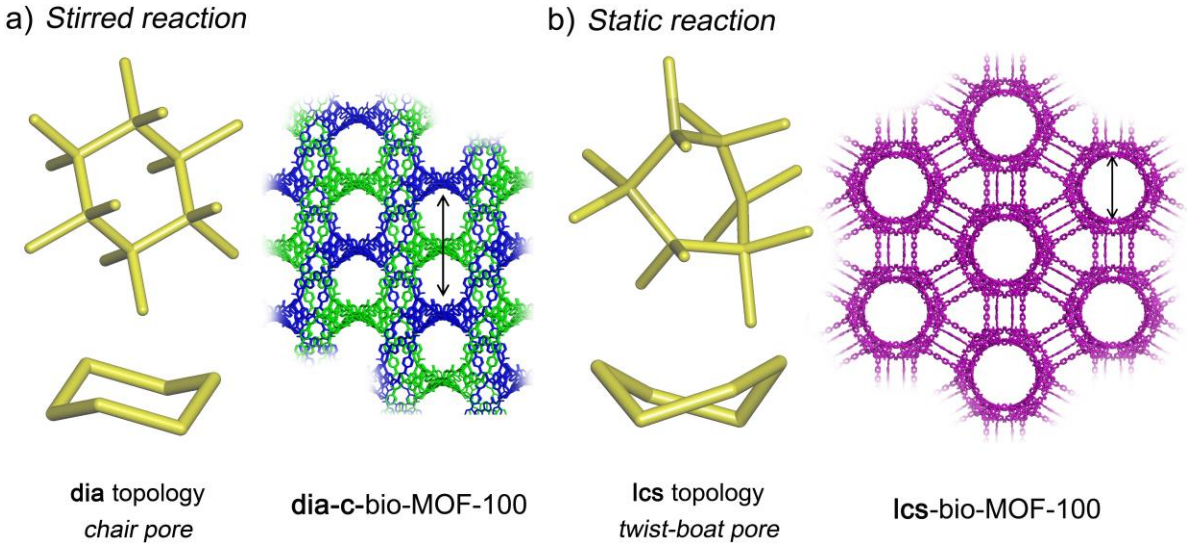

Figure 3. Representations of the two bio-MOF-100 polymorphs: a) interpenetrated **dia-c** form with a chair conformation of the hexagonal pores and b) lcs form showing the twist-boat conformation of the hexagonal pores. The black arrow points the 2.8 nm pores of the **lcs** and the ideally non-catenated **dia-c** forms; the 1.4 nm pores of the experimentally observed **dia-c** form represents half the arrow.

These bio-MOFs prepared under different synthetic conditions are polymorphs and represent two of a large number of framework topologies with linearly-bridged tetrahedral nodes. The relationship between tetrahedral coordination frameworks has been studied computationally and experimentally.[49,50] For the classic tetrahedral node-based $Zn(CN)_2$ framework,[51] different framework topologies with similar energies of formation have been postulated,[49] with the potential for reconstructive transformation to occur under pressure from the most stable doubly-interpenetrated diamondoid phase to other non-interpenetrated topologies.[50] With little difference between the energies of formation for these phases, many of these frameworks should be accessible as metastable materials provided that an appropriate synthetic pathway can be identified.

bio-MOF-100, formed by linearly-bridged tetrahedral ZABU nodes, can be considered as expanded analogues of the archetypical $Zn(CN)_2$ family. Here the synthetic pathways of the two isomeric frameworks differ in the rate of formation. Rapid precipitation from stirred reactions yields the interpenetrated **dia-c**-bio-MOF-100, analogous to the most stable form of $Zn(CN)_2$.[49] Slow crystallization under static conditions yields the previously reported **lcs-**bio-MOF-100.[35] Although clearly important, stirring is infrequently explored as a synthetic variable for MOFs; the static conditions, that more frequently yield large crystals for which structure determination from single crystal X-ray diffraction is routine, are overwhelmingly favored. As the reaction rate and local concentration of the ZABU nodes during the MOF synthesis may play an important role in determining which bio-MOF phase is formed; further adjusting the reaction concentrations or alternative synthetic approaches (e.g. microwave methods) may yield yet other 4-connected polymorphs.[52]

Notably, these two bio-MOF-100 framework isomers are not related *via* a simple distortion or displacement; the topological transformation can only be achieved by breaking, re-orienting,

and re-coordinating a large fraction of metal-ligand bonds within the MOF. Interestingly, resuspending the interpenetrated **dia-c**-bio-MOF-100 in *N*,*N*-dimethylformamide (DMF) or stirred solutions of BPDC ligands in DMF, afforded partial conversion to the non-interpenetrated **lcs**-bio-MOF-100 (see ESI). This transformation between framework isomers involves substantial reconstruction, not only to form a different topology but one with half the framework density. This reduction in framework density contrasts with the behavior observed upon synthesis of zeolites and other open frameworks,[53-54] whereby extended reaction times and contact with the reaction solution leads to denser phases. Thermochemistry has shown that the lower density frameworks are less stable (with higher heats of formation) than their dense relations.[34] While loss of catenation with no change in topology has been previously described,[16] in bio-MOF-100 this transformation is multifaceted; not only there is a change in interpenetration but also in topology. This MOF rearrangement occurs at room temperature and does not cause framework collapse nor evolution of intermediates.

Further exploring this topological transformation mediated by solvent, the native BPDC ligands within bio-MOF-100 were exchanged by iridium complexes (IrL) in solution. SALE using the denser **dia-c** MOF were remarkable efficient, proceeding highly efficiently from 5 to 45 mol% IrL incorporation at room temperature (Table 1, Figure 4). In all cases, the fraction of ligand exchanged can be controlled by tuning the concentration of the IrL solutions, being all the IrL in solution incorporated into the MOF. In contrast, ligand exchanges on **lcs**-bio-MOF-100 require a large excess of the ligand and/or higher temperatures.[28] Our results, showing ligand exchanges that are higher than those achieved in larger pore MOFs, could indicate that MOFs having dynamic structures are highly susceptible to post-synthesis modifications (e.g. labile Zn-N bonds within ZABU, flexible triplex BPDC ligand struts connecting the MOF nodes). Attempts to prepare IrL-

containing bio-MOF-100s directly[23] or by post-synthetically binding iridium complexes to bipyridyl-derived MOFs were not successful (see ESI). Incorporations of more than 50 mol% of IrL within the MOFs resulted in a drop in ligand exchange efficiency and loss of AD, together with an occurrence of a secondary zinc phase composed of paddle–wheel nodes (see ESI, Figure S6). Unlike in other dense MOFs,[23, 36] demetallation of IrL was not detected by ^{1}H NMR spectroscopic analyses on digested MOFs.

Table 1. Chemical composition and bio-MOF-100 phases of pristine controls and IrL-exchanged samples.

Sample	IrL (mol%)	IrL : BPDC[a]	AD[b]	bio-MOF-100
pristine	0	0 : 3.0	3.9	**dia-c**
pristine	0	0 : 3.0	4.0	**lcs**
5IrL	4.8	0.2 : 2.8	3.9	**dia-c** + **lcs**
10IrL	8.3	0.3 : 2.7	4.1	**dia-c**
2x5IrL[c]	8.3	0.3 : 2.7	3.7	**lcs**
15IrL	14.2	0.5 : 2.5	4.0	**dia-c**
3x5IrL[c]	13.8	0.4 : 2.6	3.4	**lcs**
20IrL	18.0	0.5 : 2.5	3.6	**dia-c**
35IrL	32.0	1.0 : 2.0	3.3	**dia-c**
50IrL	44.8	1.4 : 1.6	3.2	**dia-c**

[a]IrL to BPDC ratio referred to 3 per triplex strut in bio-MOF-100. [b]Expected value is 4 for pristine bio-MOF-100. [c]Samples prepared through successive SALE cycles are referred as *n*x5IrL, where n is the number SALE cycles performed using 5 mol% IrL solutions.

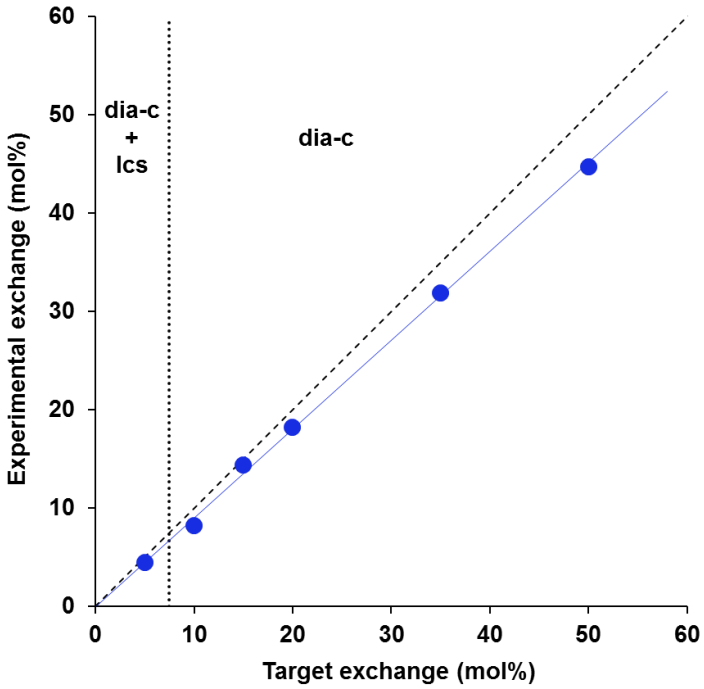

Figure 4. Experimental (blue dots) *versus* target (black dashed line) ligand exchange by IrL complexes on bio-MOF-100. The black dotted line indicates the exchange conditions under which the topological transformation from **dia-c** to **lcs** phases is observed

Interestingly, transformation from **dia-c-** into **lcs-**bio-MOF-100 was also observed during ligand exchange when low concentrated solutions of IrL were used (sample 5IrL, Figure 5b). When using intermediate concentrations, the **dia-c**–framework is retained and the ligand exchange occurs highly efficiently up to ca. 45 mol% (sample 50IrL, Table 1, Figure 5b). PDF data show that the local structure of the ZABU nodes is retained through ligand exchange (Figure 5c). XRD data show good crystallinity for all materials (Figure 5b).

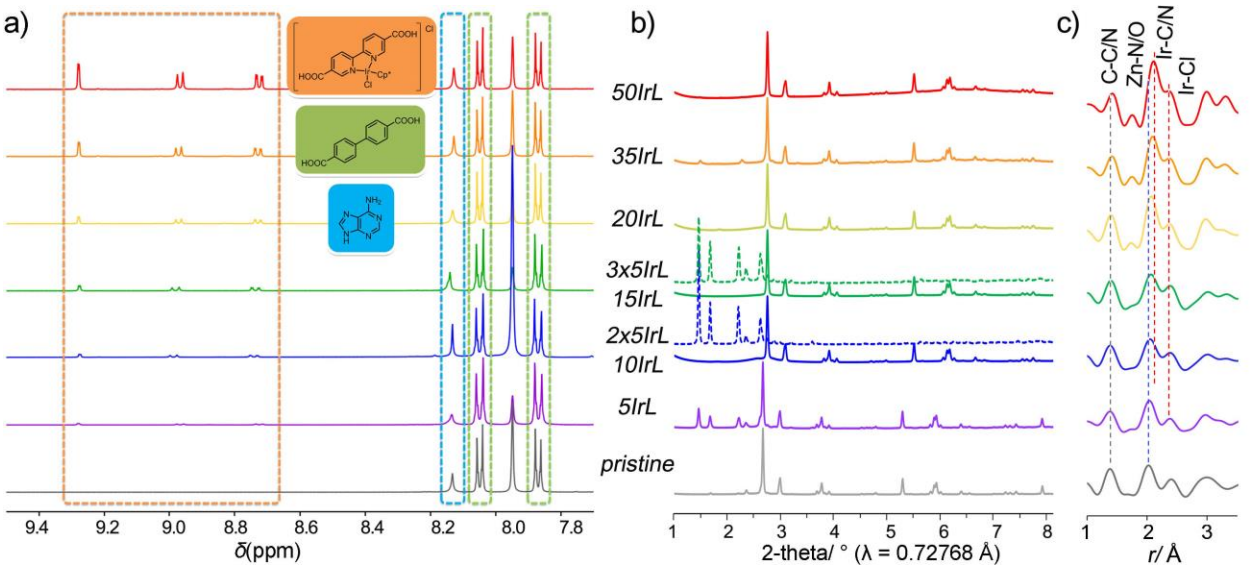

Figure 5. a) ^{1}H NMR spectroscopy analyses performed on the digested samples, b) PXRD data collected for **lcs**-bio-MOF-100 (dashed line) and **dia-c**-bio-MOF-100 (solid line), and c) detail of the total PDF profiles of the IrL-containing MOFs and pristine bio-MOF-100.

The observation that transformation between bio-MOF-100 polymorphs occurs during SALE followed by a 5 mol% ligand exchange raised the question of whether this structural transformation could be applied iteratively to reach higher functionalizations of the open form **lcs**-bio-MOF-100. Successive SALE-ing of the pristine **dia-c**-MOF, with 5 mol% IrL solutions afforded fully transformation into the non-interpenetrated **lcs**-MOF together with highly efficient ligand exchange (Table 1, samples *n*x5IrL). Crystalline MOFs containing IrL were obtained after multiple SALE cycles (Figure 5). As an example, samples with 15% of ligands substituted by IrL are discussed. Starting from a sample of pristine **dia-c**–form, exchanges performed via 3 SALE cycles using 5 mol% IrL solutions yielded to crystalline samples of the open **lcs**–form (sample 3x5IrL, Figure 6a), while performing a single SALE exchange using a 15 mol% IrL solution locked the **dia-c**-MOF (sample 15IrL, Figure 6b). The resulting materials had similar framework compositions (Table 1). Thermal stability of these two 15 mol% IrL-containing bio-MOF-100

polymorphs was assessed by thermogravimetric analyses (TGA), indicating the **lcs**-MOF to be thermally more stable than its dense **dia-c**–analogue. As shown in Figure 6, the **lcs**–phase features a single sharp differential TGA (dTGA) endothermic peak at ~480 ºC linked to the framework decomposition; the **dia-c**–form shows a main broad decomposition dTGA peak at ~420 ºC and an additional peak at ~500 ºC. Broadness of the dTGA signals observed for **dia-c**-bio-MOF-100 corroborates the structural disorder linked to this polymorph. The subtle feature below ~200 ºC, corresponding to solvent elimination from the pores, is more pronounced in **lcs**-bio-MOF-100, in agreement with the presence of an open framework.

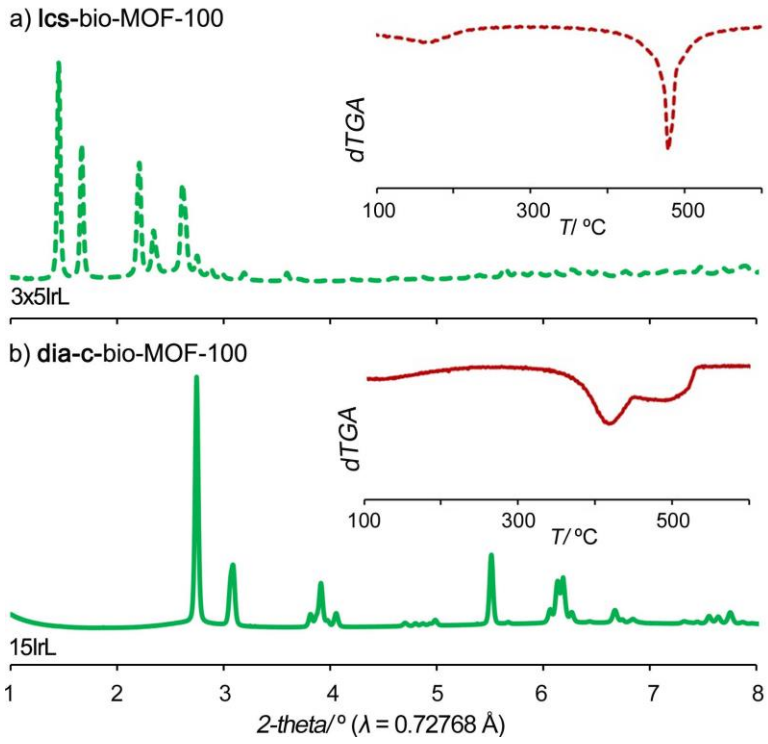

Figure 6. PXRD and dTGA (inset) data for a) 3x5IrL (low concentration regime, three SALE cycles), and b) 15IrL (intermediate concentrations regime, single SALE).

The solvent-mediated topological transformation from **dia-c**– to **lcs**–MOFs can be coupled to decoration of the framework under mild conditions. These cooperative structural and chemical

reconstructive processes found in bio-MOF-100 do not afford framework collapsing nor MOF dissolution (see in ESI a video recorded during the complete SALE process for 5IrL samples). Both bio-MOF-100 phases, featuring different densities and topologies, show adaptability to remarkable transformations of the framework. This intrinsic behavior of bio-MOF-100 would suggest the local nature of its dynamism, which may arise from the composite triplex ligand struts this MOF is composed of. During SALE, the temporary loss of one or two ligands may trigger the occurrence of structural transformations within the framework without collapsing.

The efficiency of the ligand exchange observed for both bio-MOF-100 framework isomers may be facilitated by the lower pK_a value of the H_2IrL complex compared to the metal-free linker combined to the structural dynamism of this MOF. On one hand, the difference of pK_a values between the iridium metallolinkers and the organic linkers may favor the acid-base reaction between them resulting in incorporation of IrL to the framework. On the other hand, the lability of the Zn–N/O bonds within the MOF nodes may explain the unsuspected mild conditions needed for the exchange –no excess, room temperature–. The incorporation of IrL in amounts higher than 50 mol% did not proceed cleanly under the studied conditions due protonation of the AD ligands within the nodes and the formation of a different crystalline phase (see ESI).

Combined PDF and Extended X-ray absorption fine structure (EXAFS) analyses were applied to assess the local structure and spatial isolation of the iridium complexes within the MOFs. While EXAFS is a chemical-specific technique widely used to study MOFs, it is not a very conclusive method to determine metal-metal interactions if occurrence of disorder. PDF, alternatively, providing atom-atom distances for all the atoms present in a material, can be a better technique to probe metal interactions in metal-modified MOFs. The presence of well-defined IrL sites within the bio-MOF-100 frameworks was confirmed by applying Ir L_{III}-edge EXAFS and

differential PDF (dPDF) analyses. The total PDFs for the pristine and the IrL-containing bio-MOF-100s are dominated by the more abundant Zn-atom distances involving the ZABU nodes (Figure 2a. see ESI). dPDFs, calculated by subtracting the PDF of the pristine MOF to that of the IrL-containing sample, showed the appearance of a new contribution at ~2.20 Å associated with Ir–C/N bonds from the iridium complex (Figure 7a). An additional broad contribution is determined at ~2.35 Å, linked to Ir–Cl bonds. The peak intensity of these contributions progressively increases with higher ligand exchanged by IrL.

Additionally, dPDF data did not show evidence for formation of iridium aggregates or secondary phases (i.e. IrO_2); consistent with the single-site nature of the iridium sites (see ESI, Figures S15 and S16). The coordination environment and the oxidation state of the IrL complexes within bio-MOF-100 were further confirmed by Ir L_{III}-edge EXAFS and XANES, respectively (see ESI, Figures S17 and S18). Furthermore, dPDFs of the MOFs modified with significant amounts of IrL (i.e. more than one BPDC ligand exchanged by IrL within each BPDC triplet) (see Table 1, samples 35 IrL and 50IrL) showed contributions at ~6.6 Å and ~8.3 Å which correspond to Ir…C and Ir…Ir interactions within the triplex struts in bio-MOF-100, respectively (Figure 7b).

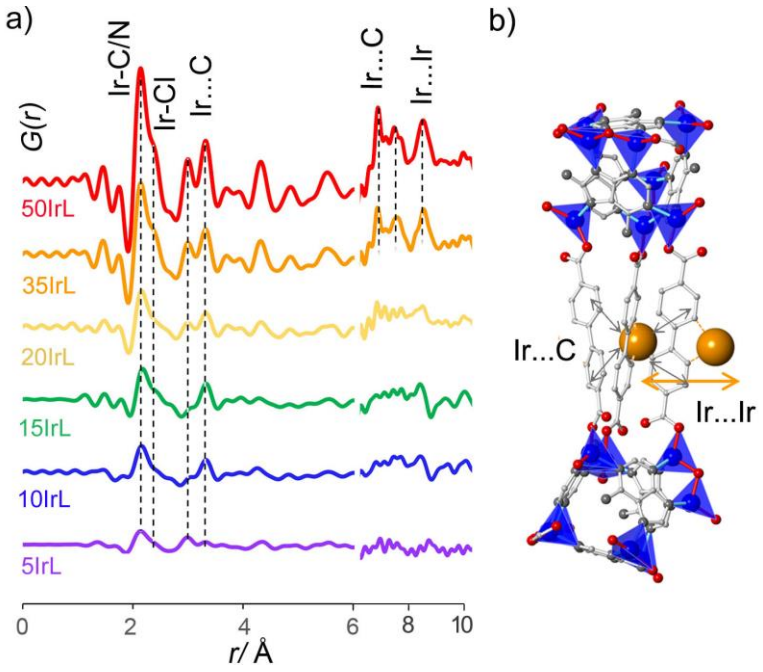

Figure 7. a) Detail of the dPDFs for MOFs exchanged with IrL showing new distances linked to iridium complexes within the frameworks, and b) triplex strut on bio-MOF-100 functionalized with two iridium sites.

CONCLUSIONS

We report here the unexpected topological transformation of a novel framework isomer of bio-MOF-100 into its known phase by doubling the pore volume, which occurs under conditions relevant for post-synthesis modifications. This structural transformation is a reconstructive process, involving breaking/forming of metal-ligand bonds and re-assembling of the building blocks into a different MOF architecture. The interpenetrated **dia-c**-bio-MOF-100 reported in this work has a different topology than the originally reported scaffold, **lcs**-bio-MOF-100. Formation of these two phases can be controlled by the nucleation rate used during the synthesis. We have shown that the topological transformation of bio-MOF-100 can be coupled to chemical decorations of the framework using SALE. Following this method and starting from the pristine dense **dia-c**

phase, open **lcs**-bio-MOF-100 was prepared and functionalized in-situ with an iridium complex (IrL). Alternatively, the **dia-c** MOF could be modified with wide-ranging amounts of IrL up to cc. 50 mol%. Controlling the pH of the solutions used for SALE (e.g. using and additional base or a buffer solution) could allow higher ligand exchanges in bio-MOF-100. All ligand exchanges occurred quantitatively at room temperature, with no need of excess of the iridium complex. We anticipate similar efficiencies using other metal complexes. While being MOFs commonly regarded as static frameworks, mostly driven by a traditional understanding of crystallinity, our work demonstrates that these materials are highly dynamic. This vision could help understanding MOFs as adaptable media amenable to architectural modifications rather than immovable solids.

ACKNOWLEDGMENTS

This project was supported by U.S. Department of Energy, Office of Science, Office of Basic Energy Sciences, under Contract No. DE-AC02-06CH11357 and the Knut and Alice Wallenberg Foundation, the Swedish Research Council (VR) and the Swedish Governmental Agency for Innovation Systems (VINNOVA) through the Berzelii Centre EXSELENT on Porous Materials. Work done at Argonne was performed using the Advanced Photon Source, a U.S. Department of Energy (DOE) Office of Science User Facility operated for the DOE Office of Science by Argonne National Laboratory under Contract No. DE-AC02-06CH11357. B.M.-M. acknowledges VINNOVA for a VINNMER grant. A.E.P.P. thanks Dr Andrey A. Yakovenko for helpful discussions on structure envelope analyses. A.E.P.P. acknowledges a Beatriu de Pinós fellowship (BP-DGR 2014) from Catalan Agency for Administration of University and Research (AGAUR).

ASSOCIATED CONTENT

Supporting Information

Details of the structure determination of the **dia-c**-bio-MOF-100, post-synthesis SALE modifications with IrL on bio-MOF-100, ^{1}H NMR spectroscopy, PDF, XAS, PXRD analyses and TGA data on bio-MOF-100 materials, and formation of a paddle-wheel zinc framework under SALE conditions targeting more than 50 mol% exchange. This material is available free of charge via the Internet at http://pubs.acs.org.

REFERENCES

1. Alezi, D.; Belmabkhout, Y.; Suyetin, M.; Bhatt, P. M.; Weseliński, Ł. J.; Solovyeva, V.; Adil, K.; Spanopoulos, I.; Trikalitis, P. N.; Emwas, A.-H.; Eddaoudi, M., MOF Crystal Chemistry Paving the Way to Gas Storage Needs: Aluminum-Based soc-MOF for CH4, O2, and CO2 Storage. *J. Am. Chem. Soc.* **2015,** *137*, 13308-13318.

2. Eddaoudi, M.; Kim, J.; Rosi, N.; Vodak, D.; Wachter, J.; O'Keeffe, M.; Yaghi, O. M., *Science.* **2002,** *295*, 469-472.

3. Mondloch, J. E.; Katz, M. J.; Isley Iii, W. C.; Ghosh, P.; Liao, P.; Bury, W.; Wagner, G. W.; Hall, M. G.; DeCoste, J. B.; Peterson, G. W.; Snurr, R. Q.; Cramer, C. J.; Hupp, J. T.; Farha, O. K., Destruction of chemical warfare agents using metal–organic frameworks. *Nat. Mater.* **2015,** *14*, 512-516.

4. Barea, E.; Montoro, C.; Navarro, J. A. R., Toxic gas removal - metal-organic frameworks for the capture and degradation of toxic gases and vapours. *Chem. Soc. Rev.* **2014,** *43*, 5419-5430.

5. Horcajada, P.; Chalati, T.; Serre, C.; Gillet, B.; Sebrie, C.; Baati, T.; Eubank, J. F.; Heurtaux, D.; Clayette, P.; Kreuz, C.; Chang, J.-S.; Hwang, Y. K.; Marsaud, V.; Bories, P.-N.; Cynober, L.; Gil, S.; Ferey, G.; Couvreur, P.; Gref, R., Porous metal-organic-framework nanoscale carriers as a potential platform for drug delivery and imaging. *Nat. Mater.* **2010,** *9*, 172-178.

6. Lu, K.; He, C.; Lin, W., Nanoscale Metal–Organic Framework for Highly Effective Photodynamic Therapy of Resistant Head and Neck Cancer. *J. Am. Chem. Soc.* **2014,** *136*, 16712-16715.

7. Lu, K.; He, C.; Guo, N.; Chan, C.; Ni, K.; Weichselbaum, R. R.; Lin, W., Chlorin-Based Nanoscale Metal–Organic Framework Systemically Rejects Colorectal Cancers via Synergistic Photodynamic Therapy and Checkpoint Blockade Immunotherapy. *J. Am. Chem. Soc.* **2016,** *138*, 12502-12510.

8. Ji, P.; Manna, K.; Lin, Z.; Urban, A.; Greene, F. X.; Lan, G.; Lin, W., Single-Site Cobalt Catalysts at New Zr8(μ2-O)8(μ2-OH)4 Metal-Organic Framework Nodes for Highly Active Hydrogenation of Alkenes, Imines, Carbonyls, and Heterocycles. *J. Am. Chem. Soc.* **2016,** *138*, 12234-12242.

9. Lee, J.; Farha, O. K.; Roberts, J.; Scheidt, K. A.; Nguyen, S. T.; Hupp, J. T., Metal-organic framework materials as catalysts. *Chem. Soc. Rev.* **2009,** *38*, 1450-1459.

10. Li, Z.; Peters, A. W.; Bernales, V.; Ortuño, M. A.; Schweitzer, N. M.; DeStefano, M. R.; Gallington, L. C.; Platero-Prats, A. E.; Chapman, K. W.; Cramer, C. J.; Gagliardi, L.; Hupp, J. T.; Farha, O. K., Metal–Organic Framework Supported Cobalt Catalysts for the Oxidative Dehydrogenation of Propane at Low Temperature. *ACS Cent. Sci.*, **2017**, 3, 31–38.

11. Makal, T. A.; Yakovenko, A. A.; Zhou, H.-C., Isomerism in Metal–Organic Frameworks: "Framework Isomers". *J. Phys. Chem. Lett.* **2011,** *2*, 1682-1689.

12. Brozek, C. K.; Michaelis, V. K.; Ong, T.-C.; Bellarosa, L.; López, N.; Griffin, R. G.; Dincă, M., Dynamic DMF Binding in MOF-5 Enables the Formation of Metastable Cobalt-Substituted MOF-5 Analogues. *ACS Cent. Sci.*, **2015,** *1*, 252-260.

13. Schneemann, A.; Bon, V.; Schwedler, I.; Senkovska, I.; Kaskel, S.; Fischer, R. A., Flexible metal-organic frameworks. *Chem. Soc. Rev.* **2014,** *43*, 6062-6096.

14. Jiang, X.; Duan, H.-B.; Khan, S. I.; Garcia-Garibay, M. A., Diffusion-Controlled Rotation of Triptycene in a Metal–Organic Framework (MOF) Sheds Light on the Viscosity of MOF-Confined Solvent. *ACS Cent. Sci.* **2016,** *2*, 608-613.

15. Platero-Prats, A. E.; Mavrandonakis, A.; Gallington, L. C.; Liu, Y.; Hupp, J. T.; Farha, O. K.; Cramer, C. J.; Chapman, K. W., Structural transitions of the metal-oxide nodes within metal-

organic frameworks: On the local structures of NU-1000 and UiO-66. *J. Am. Chem. Soc.* **2016,** *138*, 4178–4185.

16. Choi, S. B.; Furukawa, H.; Nam, H. J.; Jung, D.-Y.; Jhon, Y. H.; Walton, A.; Book, D.; O'Keeffe, M.; Yaghi, O. M.; Kim, J., Reversible Interpenetration in a Metal–Organic Framework Triggered by Ligand Removal and Addition. *Angew. Chem. Int. Ed.* **2012,** *51*, 8791-8795.

17. Serre, C.; Millange, F.; Thouvenot, C.; Noguès, M.; Marsolier, G.; Louër, D.; Férey, G., Very Large Breathing Effect in the First Nanoporous Chromium(III)-Based Solids: MIL-53 or $CrIII(OH)\cdot\{O_2C{-}C_6H_4{-}CO_2\}\cdot\{HO_2C{-}C_6H_4{-}CO_2H\}_x\cdot H_2O_y$. *J. Am. Chem. Soc.* **2002,** *124*, 13519-13526.

18. Mukherjee, S.; Joarder, B.; Manna, B.; Desai, A. V.; Chaudhari, A. K.; Ghosh, S. K., Framework-Flexibility Driven Selective Sorption of p-Xylene over Other Isomers by a Dynamic Metal-Organic Framework. *Scientific Reports* **2014,** *4*, 5761.

19. Platero‐Prats, A. E.; de la Peña‐O'Shea, V.; Snejko, N.; Monge, Á.; Gutiérrez‐Puebla, E., Dynamic calcium metal‐organic framework acts as a selective organic solvent sponge. *Chem. Eur. J.* **2010,** *16*, 11632-11640.

20. Mondloch, J. E.; Bury, W.; Fairen-Jimenez, D.; Kwon, S.; DeMarco, E. J.; Weston, M. H.; Sarjeant, A. A.; Nguyen, S. T.; Stair, P. C.; Snurr, R. Q.; Farha, O. K.; Hupp, J. T., Vapor-Phase Metalation by Atomic Layer Deposition in a Metal–Organic Framework. *J. Am. Chem. Soc.* **2013,** *135*, 10294-10297.

21. Kim, I. S.; Borycz, J.; Platero-Prats, A. E.; Tussupbayev, S.; Wang, T. C.; Farha, O. K.; Hupp, J. T.; Gagliardi, L.; Chapman, K. W.; Cramer, C. J.; Martinson, A. B. F., Targeted Single-Site MOF Node Modification: Trivalent Metal Loading via Atomic Layer Deposition. *Chem. Mat.* **2015,** *27*, 4772-4778.

22. Gallington, L. C.; Kim, I. S.; Liu, W.-G.; Yakovenko, A. A.; Platero-Prats, A. E.; Li, Z.; Wang, T. C.; Hupp, J. T.; Farha, O. K.; Truhlar, D. G.; Martinson, A. B. F.; Chapman, K. W., Regioselective Atomic Layer Deposition in Metal–Organic Frameworks Directed by Dispersion Interactions. *J. Am. Chem. Soc.* **2016,** *138*, 13513-13516.

23. Platero-Prats, A. E.; Bermejo Gómez, A.; Samain, L.; Zou, X.; Martín-Matute, B., The First One-Pot Synthesis of Metal–Organic Frameworks Functionalised with Two Transition-Metal Complexes. *Chem. Eur. J.* **2015,** *21*, 861-866.

24. Kim, M.; Cahill, J. F.; Su, Y.; Prather, K. A.; Cohen, S. M., Postsynthetic ligand exchange as a route to functionalization of 'inert' metal-organic frameworks. *Chem. Sci.* **2012,** *3*, 126-130.

25. Kim, M.; Cahill, J. F.; Fei, H.; Prather, K. A.; Cohen, S. M., Postsynthetic Ligand and Cation Exchange in Robust Metal–Organic Frameworks. *J. Am. Chem. Soc.* **2012,** *134*, 18082-18088.

26. Liu, C.; Luo, T.-Y.; Feura, E. S.; Zhang, C.; Rosi, N. L., Orthogonal Ternary Functionalization of a Mesoporous Metal–Organic Framework via Sequential Postsynthetic Ligand Exchange. *J. Am. Chem. Soc.* **2015,** *137*, 10508-10511.

27. Liu, C.; Zeng, C.; Luo, T.-Y.; Merg, A. D.; Jin, R.; Rosi, N. L., Establishing Porosity Gradients within Metal–Organic Frameworks Using Partial Postsynthetic Ligand Exchange. *J. Am. Chem. Soc.* **2016,** *138*, 12045-12048.

28. Li, T.; Kozlowski, M. T.; Doud, E. A.; Blakely, M. N.; Rosi, N. L., Stepwise Ligand Exchange for the Preparation of a Family of Mesoporous MOFs. *J. Am. Chem. Soc.* **2013,** *135*, 11688-11691.

29. Karagiaridi, O.; Bury, W.; Mondloch, J. E.; Hupp, J. T.; Farha, O. K., Solvent-Assisted Linker Exchange: An Alternative to the De-Novo Synthesis of Unattainable Metal–Organic Frameworks. *Angew. Chem. Int. Ed.* **2014,** *53*, 4530-4540.

30. Xu, Y.; Vermeulen, N. A.; Liu, Y.; Hupp, J. T.; Farha, O. K., SALE-Ing a MOF-Based "Ship of Theseus." Sequential Building-Block Replacement for Complete Reformulation of a Pillared-Paddlewheel Metal-Organic Framework. *Eur. J. Inorg. Chem.* **2016,** *27*, 4345-4348.

31. Du, S. M.; Wang, H.; Tse-Dinh, Y.-C.; Seeman, N. C., Topological Transformations of Synthetic DNA Knots. *Biochemistry* **1995,** *34*, 673-682.

32. Yamamoto, T.; Yagyu, S.; Tezuka, Y., Light- and Heat-Triggered Reversible Linear–Cyclic Topological Conversion of Telechelic Polymers with Anthryl End Groups. *J. Am. Chem. Soc.* **2016,** *138*, 3904-3911.

33. Clever, G. H., Molecular topology: Star-crossed self-assembly. *Nat. Chem.* **2014,** *6*, 950-952.

34. Hughes, J. T.; Bennett, T. D.; Cheetham, A. K.; Navrotsky, A., Thermochemistry of Zeolitic Imidazolate Frameworks of Varying Porosity. *J. Am. Chem. Soc.* **2013,** *135*, 598-601.

35. An, J.; Farha, O. K.; Hupp, J. T.; Pohl, E.; Yeh, J. I.; Rosi, N. L., Metal-adeninate vertices for the construction of an exceptionally porous metal-organic framework. *Nat. Commun.* **2012,** *3*, 604.

36. Platero-Prats, A. E.; Gómez, A. B.; Chapman, K. W.; Martín-Matute, B.; Zou, X., Functionalising metal–organic frameworks with metal complexes: the role of structural dynamics. *CrystEngComm* **2015,** *17*, 7632-7635.

37. Le Bail, A.; Duroy, H.; Fourquet, J. L., Ab-initio structure determination of LiSbWO6 by X-ray powder diffraction. *Mat. Res. Bull.* **1988,** *23*, 447-452.

38. Bruker AXS, **2005**. Karlsruhe, Germany.

39. Sisak, D.; Baerlocher, C.; McCusker, L. B.; Gilmore, C. J., Optimizing the input parameters for powder charge flipping. *J. Appl. Cryst.* **2012,** *45*, 1125-1135.

40. Palatinus, L.; Chapuis, G., SUPERFLIP - a computer program for the solution of crystal structures by charge flipping in arbitrary dimensions. *J. Appl. Cryst.* **2007,** *40*, 786-790.

41. Accelrys Software Inc., Release 4.5 , San Diego: Accelrys Software Inc., **2007**.

42. Blatov, V. A., *IUCr Comput. Comm. Newslett.* **2006,** *7*.

43. Alexandrov, E. V.; Blatov, V. A.; Kochetkov, A. V.; Proserpio, D. M., Underlying nets in three-periodic coordination polymers: topology, taxonomy and prediction from a computer-aided analysis of the Cambridge Structural Database. *CrystEngComm* **2011,** *13*, 3947-3958.

44. O'Keeffe, M.; Yaghi, O. M., Deconstructing the Crystal Structures of Metal–Organic Frameworks and Related Materials into Their Underlying Nets. *Chem. Rev.* **2012,** *112*, 675-702.

45. Juhas, P.; Davis, T.; Farrow, C. L.; Billinge, S. J. L., PDFgetX3: a rapid and highly automatable program for processing powder diffraction data into total scattering pair distribution functions. *J. Appl. Cryst.* **2013,** *46*, 560-566.

46. Wojdyr, M., Fityk: a general-purpose peak fitting program. *J. Appl. Cryst.* **2010,** *43*, 1126-1128.

47. Newville, M., IFEFFIT: interactive EXAFS analysis and FEFF fitting. *J. Synchrotron Rad.* **2001,** *8,* 322-324.

48. Ravel, B.; Newville, M. ATHENA, A., HEPHAESTUS: data analysis for X-ray absorption spectroscopy using IFEFFIT. *J. Synchrotron Rad.* **2005,** 12, 537-541.

49. Trousselet, F.; Boutin, A.; Coudert, F.-X., Novel Porous Polymorphs of Zinc Cyanide with Rich Thermal and Mechanical Behavior. *Chem. Mater.* **2015,** *27*, 4422-4430.

50. Lapidus, S. H.; Halder, G. J.; Chupas, P. J.; Chapman, K. W., Exploiting High Pressures to Generate Porosity, Polymorphism, And Lattice Expansion in the Nonporous Molecular Framework $Zn(CN)_2$. *J. Am. Chem. Soc.* **2013,** *135*, 7621-7628.

51. Hoskins, B. F.; Robson, R., Design and construction of a new class of scaffolding-like materials comprising infinite polymeric frameworks of 3D-linked molecular rods. A reappraisal of the zinc cyanide and cadmium cyanide structures and the synthesis and structure of the diamond-related frameworks $[N(CH_3)_4][Cu^{I}Zn^{II}(CN)_4]$ and CuI[4,4',4",4"'-tetracyanotetraphenylmethane]$BF_4.xC_6H_5NO_2$. *J. Am. Chem. Soc.* **1990,** *112*, 1546-1554.

52. ontrol experiments showed low solubility of zinc acetate dihydrate in the reaction media. Under static conditions, the local concentration of ZABU nodes in the reaction would be lower than under stirring, directing to **lcs**- or to the **dia-c** forms, respectively.

53. Platero-Prats, A. E.; de la Peña-O'Shea, V. A.; Proserpio, D. M.; Snejko, N.; Gutiérrez-Puebla, E.; Monge, Á., Insight into the SBU Condensation in Mg Coordination and Supramolecular Frameworks: A Combined Experimental and Theoretical Study. *J. Am. Chem. Soc.* **2012,** *134*, 4762-4771.

54. Carson, F.; Su, J.; Platero-Prats, A. E.; Wan, W.; Yun, Y.; Samain, L.; Zou, X., Framework Isomerism in Vanadium Metal–Organic Frameworks: MIL-88B(V) and MIL-101(V). *Cryst. Growth Des.* **2013,** *13*, 5036-5044.

Table of Content

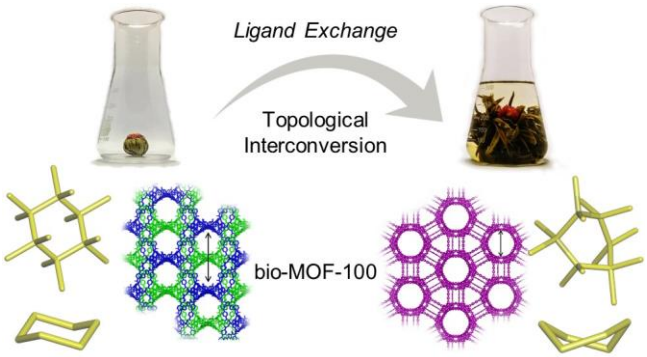

SYNOPSIS. Here we describe the topological transformation of a new framework in the bio-MOF-100 family (**dia-c**) into the known isomer (**lcs**) by doubling the pore volume, which occurs during post-synthesis ligand exchange. During this transformation, re-assembling of the MOF building blocks into a completely different framework occurs, involving breaking/forming of metal-ligand bonds. We have exploited the inherent dynamism of bio-MOF-100 by coupling controlled chemical decorations of the framework with an iridium complex to the topological change.